MIT Open Access Articles

Probing nanoantenna-directed photothermal destruction of tumors using noninvasive laser irradiation

Massachusetts Institute of Technology

DSpace@MIT

Probing nanoantenna-directed photothermal destruction of tumors using noninvasive laser irradiation

Debabrata DasGupta,[1] Geoffrey von Maltzahn,[2] Soham Ghosh,[3] Sangeeta N. Bhatia,[2,4] Sarit K. Das,[3] and Suman Chakraborty[1,a)]

[1]*Department of Mechanical Engineering, IIT Kharagpur, Kharagpur 721302, India*
[2]*Harvard-MIT Division of Health Sciences and Technology, Cambridge, Massachusetts 02142, USA*
[3]*Department of Mechanical Engineering, IIT Madras, Chennai 600036, India*
[4]*Electrical Engineering and Computer Science, MIT/Brigham and Women's Hospital, Cambridge, Massachusetts 02139, USA*

Plasmonic nanomaterials have tremendous potential to improve the tumor specificity of traditional cancer ablation practices, yet little effort has been directed toward quantitatively understanding their photothermal energy conversion in tumor tissues. In the present work, we develop a predictive model for plasmonic nanomaterial assisted tumor destruction under extracorporeal laser irradiation. Instead of appealing to heuristically based laser intensification models with tunable, tissue absorption and scattering coefficients, we consider fundamental characteristics of optoelectrothermal energy conversion and heat dissipation for plasmonic nanomaterials within living tumor tissues to construct a simulation tool that accurately reproduces our experimental findings, including aspects of delayed time-temperature characteristics. We believe the comprehensive modeling strategy outlined here provides a groundwork for the development of anticipatory therapeutic planning tools with individually tailored treatment plans, resulting in an ultimate benefit to ailing cancer patients. © 2009 American Institute of Physics.
[doi:10.1063/1.3271522]

The use of plasmonic nanomaterials in photothermal therapy of tumors has received increasing attention over the past few years,[1–9] primarily because of the directivity, specificity, and nonintrusive nature of the underlying treatment protocol. Tumor-targeted nanoantennas are ideally suited for many of these applications. These nanoantennas exploit the geometrically tunable surface plasmon resonance (SPR) phenomenon of metal nanoparticles, whereby external electromagnetic fields can induce the resonant oscillation of nanoparticle free electrons and allow efficient photothermal conversion of the nonradiative extinction component to heat through electron-electron and electron-phonon relaxation mechanisms.[2–9] Further, surface-modification of nanostructured plasmonic materials with polymers and targeting ligands has enabled those to evade rapid clearance from the blood stream and intravenously target tumors via unique biological tumor characteristics, thereby enabling highly specific heating of tumor cells under laser irradiation with wavelengths overlapping the nanoparticle SPR absorption regime.[2–9]

While preclinical tests with tumor-targeted nanoantennas have produced impressive results,[10] few efforts have been made to quantitatively model and predict four-dimensional temperature gradients[11] in tumors and neighboring tissues. Previously, we developed a photothermal heating model where, on system spatiotemporal scales, the details of nanoantenna energy conversion were abstracted with predefined tuning parameters prescribed in terms of macroscopic tissue absorption and scattering coefficients,[12] with an intention of mimicking the underlying microscale interactions in an upscaled physical limit by appealing to the gross

consequences of the pertinent photothermal interactions. Such considerations, however, are not physically complete in nature, since the thermophysical interactions occurring over disparate physical scales are intensely coupled with a number of significant criticalities and constraints in a rather complicated and dynamically evolving manner.

Here we outline a predictive methodology for delineating the thermal profiles in tumors subjected to metal nanoantenna assisted laser ablation. In contrast to the standard *ad hoc* approaches, macroscopic scattering and absorption coefficients corresponding to an attenuated optical energy penetration in nanorod-targeted tumor tissues are not set a-priori. Rather, we model the nanoscale optothermal interactions due to laser irradiation of tissue-embedded nanorods by appealing to the fundamental energy conversion and dissipation mechanisms pertinent to light to heat conversion *in vivo* as mediated by electrical properties of the nanostructure. With our physical considerations, we establish via model validation with experimental findings that the physics of nanostructure assisted laser-tumor interactions in living systems can be quantitatively reproduced by a comprehensive interaction model without necessitating additional fitting parameters.

Fundamentally, laser irradiation of tumor cells mediated by nanostructured materials may be conceptualized by ap-

TABLE I. Details of coefficients pertinent to temperature dependent blood perfusion.

	a (m³/kg/s)	b	f
Tumor core	5×10^{-7}	1	$=a$ for $T \leq 39$ °C
Periphery	1.67×10^{-6}	2	$=a[1+(b-1)(T-39)/6]$ for 39 °C$<T\leq45$ °C
Muscle	8.3×10^{-6}	9	$=a[b-(b-1)(T-45)/6]$ for 45 °C$<T\leq51$ °C
Skin	8.3×10^{-6}	9	$=a$ for $T>51$ °C

a)Author to whom correspondence should be addressed. Electronic mail: suman@mech.iitkgp.ernet.in.
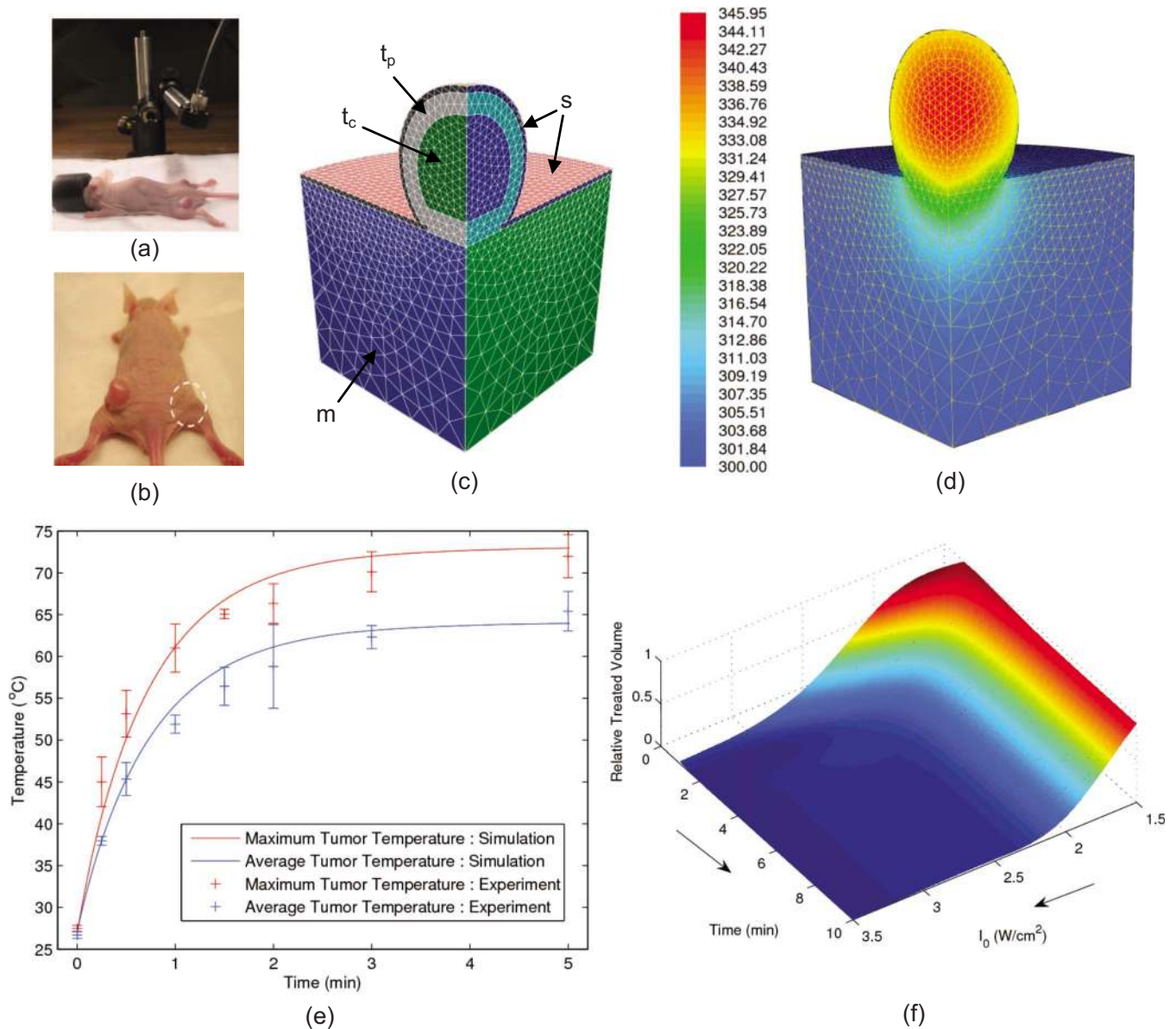
FIG. 1. (Color online) Photothermal modeling of gold nanorod tumor heating (a) The nanorod heating setup showing the tumor before irradiation with the laser (b) Mouse after photothermal destruction of the tumor (c) The computational domain showing the various layers: tumor core (t_c), tumor periphery (t_p), skin (s), and the muscle layers (m). The computational domain was tessellated using tetrahedral meshes (0.4 mm along the tumor section and graded to 0.7 mm along the bottom of the domain) (d) The temperature profile 5 min following the onset of irradiation (colorbar showing temperatures in K) at $I_0=2$ W/cm^2. (e) The measured and simulated average and maximum tumor temperatures over time (f) Time-treated volume history as a function of laser irradiation intensity (the volume is considered to be treated when the temperature reaches the ablative limit of 60 °C). Simulation data taken are as follows: $\varepsilon_0=1.8$, $\varepsilon_m=-27.2126+1.9157i$, $f_v=0.0021$, $\rho_b=0.937$ g/s/cm^3, $\phi=0.1$, $c_b=3889$ mW s/g °C, $T_b=27$ °C, $\rho=1.07$ g/s/cm^3, $c=3471$ mW s/g °C, $k=4.42$ mW/cm °C.

pealing to the electromagnetic field generated as a consequence of light-free electron interactions. As the electromagnetic field oscillates back and forth in the direction of the electrical field polarization, these electrons collectively respond to the incipient excitation. Coulombic attraction between electrons and the metal cations (or lattice) provide the necessary restoring forces for electrons in their out-of-equilibrium configurations. Consequently, there may be a transient charge displacement, and equivalently a time-dependent induced dipole moment during oscillation. Combinations of the transient electric field (**E**) generated as a consequence and the corresponding current density (**J**) in the conducting matrix gives rise to a volumetric thermal energy source, physically representing the energy dissipation rate in the nanostructure, which may be quantified as follows:[13]

$Q_{\text{laser}}=\langle\mathbf{J}\cdot\mathbf{E}\rangle_t=-1/2\,\text{Re}\{i\omega[(\varepsilon_{\text{eff}}-1)/(4\pi)]\hat{\mathbf{E}}\hat{\mathbf{E}}^*\}$, where **E** $=\text{Re}[\hat{\mathbf{E}}e^{-i\omega t}]$. Importantly, ε_{eff} is the effective dielectric constant of the nanoantenna-targeted tissue, which may be described as a function of the dielectric constant of the constituents of the tumor, i.e., an aqueous phase (ε_0) and the metallic nanostructures (ε_m), as[14] $\varepsilon_{\text{eff}}=\varepsilon_0+3\phi\varepsilon_0\{(\varepsilon_m-\varepsilon_0)/[\varepsilon_m+2\varepsilon_0-\phi(\varepsilon_m-\varepsilon_0)]\}$, where ϕ is the volume fraction of nanoparticles in the base fluid, and ε_m is a function of the wavelength.[15] Considering the field $\hat{\mathbf{E}}$ and the externally imposed field due to laser excitation ($\mathbf{E}_0$) to be proportioned on the basis of the dielectric constants of the metal and the matrix, it follows:[16] $\hat{\mathbf{E}}=[(3\varepsilon_0)/(2\varepsilon_0+\varepsilon_m)]\mathbf{E}_0$. Noting that the external laser field is related to the laser intensity, I_0, as $I_0=cE_0^2\sqrt{\varepsilon_0}/8\pi$, one may write: $Q_{\text{laser}}=-\text{Re}[i\alpha I_0]$, where α

$=[\omega(\varepsilon_{\text{eff}}-1)]/(c\sqrt{\varepsilon_0})|3\varepsilon_0/(2\varepsilon_0+\varepsilon_m)|^2$. The transience in temperature within the tumor is governed by the following differential equation: $[\partial/(\partial t)](\rho cT)+\nabla\bullet(\rho c\vec{V}T)=\nabla\bullet(k\nabla T)+f_vQ_{\text{laser}}+Q_{\text{metabolic}}+Q_{\text{blood}}+Q_{\text{phase change}}$, where f_v is the local volume fraction of nanostructures in the matrix, $Q_{\text{metabolic}}$ is the volumetric rate of metabolic heat generation, $Q_{\text{blood}}(=\rho_b w_b c_b(T_b-T))$ is the rate of blood perfusion (w_b is a temperature- and cell location dependent coefficient), and $Q_{\text{phase change}}$ is the volumetric rate of latent heat evolution/absorption.[17] We solve the governing differential equation by adopting the Finite Volume Method for spatial discretization and fully implicit approach for temporal discretization. We take the temperature and location dependence of the blood perfusion into account by considering $w_b=f(a,b)$, where the forms of the function f over different temperature ranges, as well as values of the parameter a and b are given in Table I.

In an effort to assess the predictive capabilities of the present model vis-à-vis experimental findings, we employed polyethylene glycol (PEG)-coated Au nanorods for laser aided photothermal destruction of tumors in mice. For sample preparation, highly stable, $\sim 13\times 47$ nm^2 Au nanorods with SPR at 810 nm (Nanopartz, Salt Lake City, UT) were employed.[12] Nude mice were bilaterally injected subcutaneously with $\sim 2\times 10^6$ MDA-MB-435 cells in the hind flank. After 2–3 weeks, the mice were anesthetized with isoflurane and PEG-nanorods were injected through their tail veins in a vehicle of 0.15 M NaCl, 0.1M Na phosphate buffer (pH=7.2; 20 mg Au/kg). Following vascular clearance and tumor targeting via the hyperporous angiogenic blood vessels over the course of the next 72 h, the right flanks of the mice were widely irradiated with 2 W/cm^2 laser intensity with real-time surface temperature assessment via infrared thermography (FLIR Thermacam) to facilitate comparison of model predictions against *in vivo* experimental recordings.

In order to assess the quantitative capabilities of the present model in terms of a one-to-one mapping between the laser irradiation on the nanorod-targeted tumors and the temporal evolution of temperature at different tumor locations, Fig. 1 is plotted, in which the thermal profiles at different instants of time are pictorially depicted. For experimentally delineating the distinctive influences of the nanorods, the PEG-nanorods and a saline solution were independently administered through intravenous routes into mice bearing two MDA-MB-435 tumors on opposite flanks. The saline injected mice displayed much less focal temperature increments (maximum surface temperature around 40 °C) as compared to the nanorod injected mice (maximum surface temperature around 70 °C). We obtained an excellent agreement between the present computational studies and the experimental results, as evident from Fig. 1. In addition to a correct prediction of the ablative temperature rise of a short period of characteristic time (~ 5 min), the present model aptly captures the asymptotic nature of the later transients in the temperature-time history, which will be critical for future planning of therapeutic treatment times. This enhanced capability of the present model may be attributed to the fundamentals of SPR phenomenon directly incorporated into the laser-tumor interaction model, instead of considering predefined tissue absorption characteristics. More importantly, in doing so, the present model does not necessitate the employment of tuning parameters such as scattering and absorp-

tion coefficients which makes its implementation universal over a wide range of experimental conditions. The present simulation studies also enable us to address varied input conditions and may act as a predictive tool for predesigning the therapeutic protocol based on the temperature-treated volume history [see Fig. 1(f)].

To summarize, we have developed a fundamental mathematical model for nanoantenna-assisted laser destruction of tumor cells and validated the model's temperature predictions against *in vivo* experiments. Such efforts are expected to be contributory toward the medical treatment under critical biophysical conditions, in which there is likely to be a natural emphasis on the optimization and control of various therapeutic parameters, along with the minimization of purely experience based photothermal treatment protocols. Toward that, the present study is expected to unveil a deeper understanding of physicothermal processes involved with laser-tumor interactions, by quantifying the role of irradiance, variations in electro-optical properties of the nanostructures, wavelength and exposure time on the treated volume, thereby enabling one to control the treatment by suitably regulating these parameters *a priori*. Furthermore, we believe the model presented here provides a stepping stone toward understanding the multiscale processes of photothermal ablation and opens doors toward modeling "nanosurgeries," where pulsed laser sources and nanoantennas could have the potential to generate dramatic nanoscale thermal gradients and provide single cell specificity to therapies.

[1] V. A. Mostovnikov, G. R. Mostovnikova, V. Y. Plavski, L. J. Plavskaja, and R. P. Morozova, Proc. SPIE **2370**, 541 (1995).
[2] L. R. Hirsch, R. J. Stafford, J. A. Bankson, S. R. Sershen, B. Rivera, R. E. Price, J. D. Hazle, N. J. Halas, and J. L. West, Proc. Natl. Acad. Sci. U.S.A. **100**, 13549 (2003).
[3] D. P. O'Neal, L. R. Hirsch, N. J. Halas, J. D. Payne, and J. L. West, Cancer Lett. **209**, 171 (2004).
[4] R. S. Norman, J. W. Stone, A. Gole, C. J. Murphy, and T. L. Sabo-Attwood, Nano Lett. **8**, 302 (2008).
[5] X. Huang, L. H. El-Sayed, W. Qian, and M. A. El-Sayed, J. Am. Chem. Soc. **128**, 2115 (2006).
[6] A. M. Gobin, M. H. Lee, N. J. Halas, W. D. James, R. A. Drezek, and J. L. West, Nano Lett. **7**, 1929 (2007).
[7] H. Xie, K. L. Gill-Sharp, and P. O'Neal, Nanomed. Nanotechnol. Biol. Med. **3**, 89 (2007).
[8] W. D. James, L. R. Hirsch, J. L. West, P. D. O'Neal, and J. D. Payne, J. Radioanal. Nucl. Chem. **271**, 455 (2007).
[9] E. B. Dickerson, E. C. Dreaden, X. Huang, I. H. El-Sayed, H. Chu, S. Pushpanketh, J. F. McDonald, and M. A. El-Sayed, Cancer Lett. **269**, 57 (2008).
[10] S. Lal, S. E. Clare, and N. J. Halas, Acc. Chem. Res. **41**, 1842 (2008), and the references therein.
[11] D. K. Kim, M. S. Amin, S. Elborai, S. H. Lee, Y. Koseoglu, and M. Muhammed, J. Appl. Phys. **97**, 10J510 (2005).
[12] G. von Maltzahn, J.-H. Park, A. Agrawal, N. K. Bandaru, S. K. Das, M. J. Sailor, and S. N. Bhatia, Cancer Res. **69**, 3892 (2009).
[13] A. O. Govorov, W. Zhang, T. Skeini, H. Richardson, J. Lee, and N. A. Kotov, Nanoscale Res. Lett. **1**, 84 (2006).
[14] L. Rayleigh, Philos. Mag. **34**, 481 (1892).
[15] E. D. Palik, *Handbook of Optical Constants of Solids* (Academic, New York, 1985).
[16] L. D. Landau, E. M. Lifschitz, L. D. Landau, and E. M. Lifshitz, *Electrodynamics of Continuous Media* (Pergamon, New York, 1960).
[17] R. Dua and S. Chakraborty, Comput. Biol. Med. **35**, 447 (2005).